Energy and Charge Transfer Dynamics in Fully Decorated Benzyl Ether Dendrimers and Their Disubstituted Analogues

Tai-Sang Ahn,[†] Arpornrat Nantalaksakul,[‡] Raghunath R. Dasari,[‡] Rabih O. Al-Kaysi,[†] Astrid M. Müller,[†] S. Thayumanavan,*[,‡] and Christopher J. Bardeen*[,†]

Department of Chemistry, University of California, Riverside, California 92521, and Department of Chemistry, University of Massachusetts, Amherst, Massachusetts 01003

Received: August 2, 2006; In Final Form: September 28, 2006

We examine the photophysics of a series of molecules consisting of a benzthiadiazole core surrounded by a network of benzyl ether arms terminated by aminopyrene chromophores, which function as both energy and electron donors. Three classes of molecules are studied: dendrimers whose peripheries are fully decorated with aminopyrene donors (**F**), disubstituted dendrimers whose peripheries contain only two donors (**D**), and linear analogues in which a pair of benzyl ether arms link two donors to the central core (**L**). The electronic energy transfer (EET) and charge transfer (CT) rates are determined by fluorescence lifetime measurements on the energy donors and electron acceptors, respectively. In all three types of molecules, the EET time scales as the square root of the generation number *G*, consistent with the flexible nature of the benzyl ether framework. Transient anisotropy measurements confirm that donor−donor energy hopping does not play a major role in determining the EET times. The CT dynamics occur on the nanosecond time scale and lead to stretched exponential decays, probably due to conformational disorder. Measurements at 100 °C confirm that conformational fluctuations play a role in the CT dynamics. The average CT time increases with *G* in the **L** and **D** molecules but decreases for the **F** dendrimers. This divergent behavior as *G* increases is attributed to the competing effects of larger donor−acceptor distances (which lengthen the CT time) versus a larger number of donors (which shorten the average CT time). This work illustrates two important points about light-harvesting and charge-separation dendrimers. First, the use of a flexible dendrimer framework can lead to a more favorable scaling of the EET time (and thus the light-harvesting efficiency) with dendrimer size, relative to what would be expected for a fully extended dendrimer. Second, fully decorated dendrimers can compensate for the distance-dependent slowdown in CT rate as *G* increases by providing additional pathways for the CT reaction to occur.

Introduction

Organic molecular assemblies are a potentially low-cost alternative for solar energy conversion. One approach involves using solid-state films of conjugated polymers or oligomers to mimic the function of inorganic semiconductors in traditional photovoltaic cells. A different approach is to construct large molecules which mimic the functionalities of the biological light-harvesting complex and the photosynthetic reaction center.[1,2] For example, many researchers have synthesized and characterized multichromophore dendrimers, where a single energy acceptor is surrounded by a branching network of energy donors.[3−22] This type of structure functions as an artificial light-harvester, where the energy of a single photon is rapidly transferred through the peripheral donors to the core acceptor.[23,24] These types of molecules act to concentrate the photon energy at the core, and the effective energy concentration depends on the donor−acceptor ratio. In dendrimers, the donor−acceptor ratio is increased by adding successive generations around the central core. This increase in generation also leads to an increase in the average donor−acceptor distance, however, which tends to decrease the overall light-harvesting rate. But light-harvesting represents only the first step in the photosynthetic process, which also involves the creation of a long-lived charge-separated state in order to convert photon energy into an electrochemical potential. While work on most dendrimers has concentrated on optimizing electronic energy transfer (EET) to the core, there have also been a few reports on charge transfer within dendritic architectures in both conjugated and nonconjugated systems.[25−29] We have recently reported a system that combines both electronic energy transfer (EET) and charge transfer (CT) events sequentially in the same dendrimer.[30]

The development of dendrimers which exhibit both EET and CT processes raises interesting questions as to how these different physical processes occur within the same molecule, and how each scales with dendrimer size. In the benzyl ether (BE) dendrimers studied by us previously, the EET occurs from the outer layer of donors to a single acceptor at the center of the molecule. This leads to a dependence on dendrimer size that is easily understood. As the generation *G* of the dendrimer increases, the donor layer moves outward from the core, and the average donor−acceptor separation increases. From the perspective of the peripheral donor, the only thing changing with *G* is the average distance over which EET must take place. Thus the EET time, denoted τ_{EET}, is expected to steadily increase with *G*. We then consider the core acceptor molecule which undergoes a CT reaction with one of the peripheral electron donors. As *G* increases, the average donor−acceptor separation increases, which should increase the average CT time τ_{CT} just

[†] University of California.
[‡] University of Massachusetts.

10.1021/jp0649706 CCC: $33.50
Published on Web 11/11/2006

as it increases τ_{EET}. But the total number of donors available for CT also doubles with generation. This increase in the local donor density provides more opportunities for CT to occur and would thus act to decrease average CT time for the dendrimer, τ_{CT}^{dend}. While increasing G serves only to lengthen τ_{EET}, τ_{CT}^{dend} is determined by two competing effects, and it is not easy to predict its dependence on G.

To test these qualitative ideas about the different behaviors of the EET and CT rates, we have measured both as a function of generation in a family of BE macromolecules. The BE linkages lead to highly flexible arms, and the possible role of conformational disorder can complicate any systematic interpretation of the data.[31,32] In an attempt to disentangle the roles of conformational disorder and increasing generation G, we compare the dynamics of the fully decorated dendrimers (**F**) with those of dendrimers which possess only two peripheral chromophores (**D**) and also disubstituted linear analogues (**L**), which do not have the constraints of the branched dendrimer architecture.[33] By measuring the time-resolved fluorescence dynamics of both the donor amino-pyrenes (to monitor the EET) and the acceptor benzthiadiazole (to monitor the CT quenching), we can look at how both the EET and CT rates evolve with size. We find that all three types of donor−acceptor molecules (**F**, **D**, and **L**) show a similar scaling of the EET rate with generation. As observed previously, this size scaling is consistent with that expected for flexible arms which have a distribution of conformations. The CT behavior of the three families of compounds is where a divergence is observed. As the polarity of the solvent increases, the CT quenching of the acceptor fluorescence becomes more rapid in all compounds, and the disordered conformations lead to a stretched exponential decay of the fluorescence. In the disubstituted molecules (**D**, **L**), the overall decay rate decreases with increasing generation, as expected due to the increased donor−acceptor separation. But the **F** molecules show a more rapid quenching and the opposite size dependence. Our results suggest that the increased number of donors in larger **F** dendrimers may partially offset the unavoidable effects of increased distance between donor and acceptor moieties. Fully decorated dendrimers may represent a way to optimize both the electronic energy concentration (due to the large number of donors) and the subsequent charge-separation efficiency.

Experimental Section

The molecules studied here were synthesized according to previously published methods,[33] and their structures are shown in Figure 1. For the spectroscopic measurements, the samples were dissolved in toluene, methylene chloride, and dimethylformamide (DMF) in a 1×1 cm^2 cuvette with optical densities less than 0.2. Toluene and methylene chloride were used as received while DMF was dried with molecular sieves before use. Steady-state absorption and fluorescence spectra were recorded using a Varian Cary 50 UV−vis spectrophotometer and a Spex Fluorolog fluorometer. Changing the sample concentration had no effect on the spectral shapes.

Fluorescence lifetimes were measured by exciting the samples using pulses centered at 400 nm, derived from the frequency doubled output of a 40 kHz regeneratively amplified Ti:sapphire laser system with a 150 fs pulse width. Fluences were less than 5 μJ/cm^2. The spectra and time decay of the fluorescence remained unchanged up to laser fluences of 200 μJ/cm^2. The low laser fluences used and the lack of intensity-dependent effects in the fluorescence decay both indicate that multiphoton absorption events by a single dendrimer molecule can be neglected. To purify the polarization of the excitation beam, the laser was passed through a calcite polarizer before exciting the sample. The emission of the samples was collected at 90° relative to the excitation beam. The emission was collimated and focused into a monochromator (Spectra Pro-150 spectrometer) with a 150 grooves/mm grating to disperse the spectrum before being passed to a picosecond streak camera (Hamamatsu C4334 Streakscope). The instrument response of this instrument was ~15 ps in 1 ns sweep window. A second polarizer is placed in the collimated emission and rotated relative to the excitation polarization for fluorescence anisotropy measurements.

The fluorescence spectrum of **3F** acceptor in DMF has a long-lived component, which likely originates from the red wing of the residual donor emission. The fluorescence spectrum, 20 ns after the excitation pulse, is dominated by this impurity emission. For this molecule, we have to separate the contribution of the acceptor and donor emissions in order to obtain an accurate lifetime of the acceptor. To do this, the emission spectra at each time interval are least-squares fitted to a weighted sum of acceptor and impurity spectra,[34,35]

$$S(\lambda,t) = c_{acc}(t)\, S_{acc}(\lambda) + c_{im}(t)\, S_{im}(\lambda) \qquad (1)$$

where $S(\lambda,t)$ is the measured fluorescence signal and $S_{acc}(\lambda)$ and $S_{im}(\lambda)$ are fluorescence spectra of the acceptor and impurity respectively with $c_{acc}(t)$ and $c_{im}(t)$ as their coefficients. The fluorescence spectrum of the acceptor is assumed to match the spectrum of the **2F** acceptor in DMF, which shows negligible donor emission at the longer delays. The long-lived donor component is taken to be the fluorescence spectrum measured after a 20 ns delay. The time evolution of coefficient $c_{acc}(t)$ in fluorescence lifetime measurements is taken as the true decay of the acceptor fluorescence.

Results and Discussion

1. Electronic Energy Transfer. All the BE molecular assemblies behave as collections of independent chromophores.[30,33] For example, Figure 2 shows a comparison of the absorption of the monomeric donor, the monomeric acceptor, and the **2F** dendrimer. The spectrum of the dendrimer is well-described as a superposition of the acceptor plus 8 donors, as expected based on the chemical structure of **2F**. There is no evidence for any through-bond electronic communication between the conjugated species that would lead to changes in the electronic spectra. The fluorescence spectrum of the dendrimer also consists of two well-separated emission peaks centered at ~450 nm for the donor and ~600 nm for the acceptor. We did not observe any signatures of excimer or exciplex formation for any of the compounds studied here. What is clear from the fluorescence spectrum is that the donor fluorescence is largely quenched in the dendrimers, presumably due to EET to the lower energy benzthiadiazole core. The calculated Forster radius for this donor−acceptor pair is 4.8 nm,[30] which is larger than the size of the entire dendrimer molecule.

As in our earlier paper, direct EET from the donor to the core can be quantified by simultaneously monitoring the donor decay and the growth of the acceptor emission. Figure 3 shows an example of this for the **3L** molecule, where the relatively slow EET dynamics make it easy to resolve both the donor decay and the acceptor growth. The solid lines are calculated signals given a single EET time (127 ps from Table 1) and amplitudes determined by the relative absorption coefficients at the 400 nm excitation wavelength. As in our previous studies of the fully decorated dendrimers,[30] the kinetic modeling of the

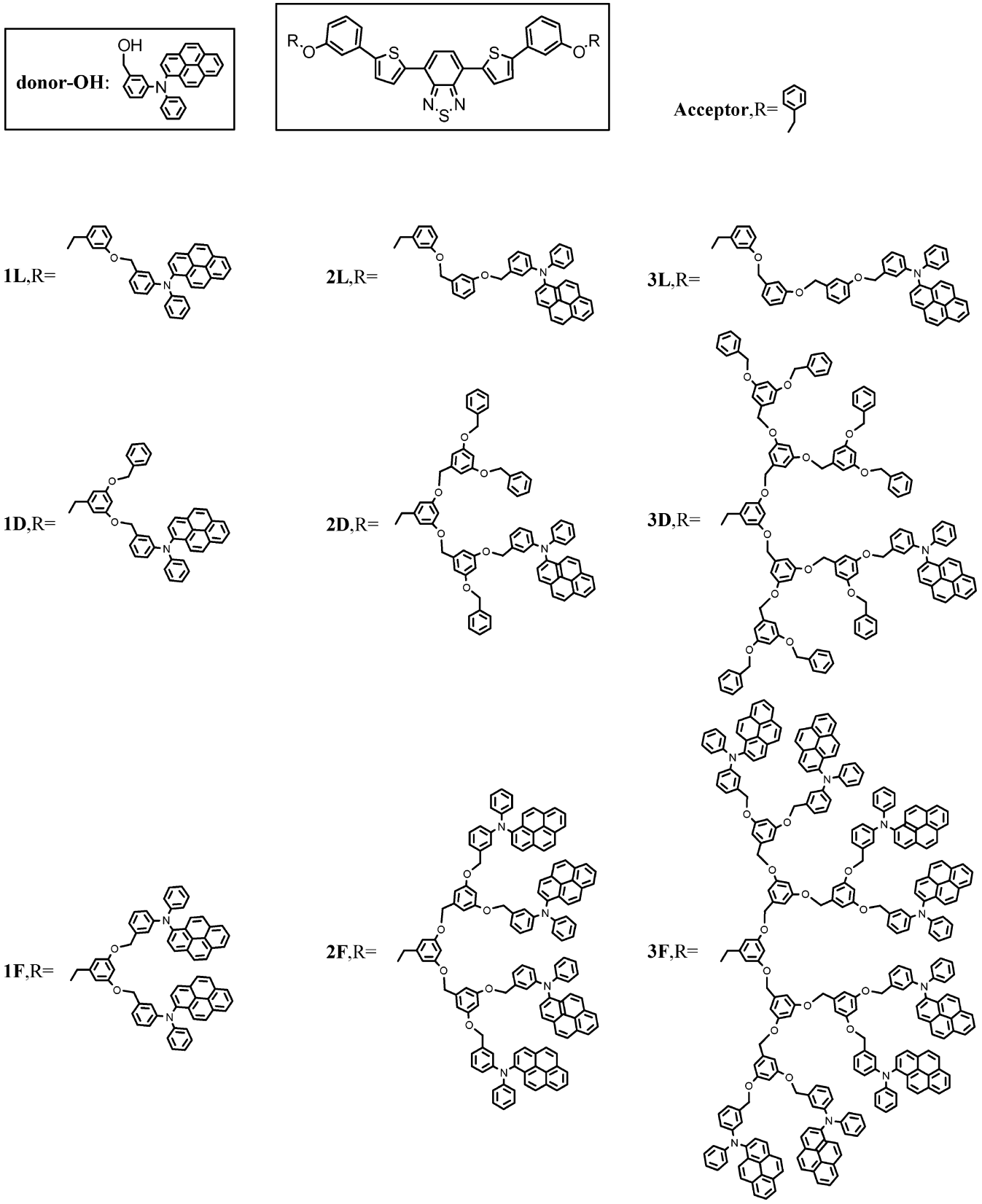

Figure 1. Structures of the BE compounds studied in this work.

wavelength-dependent fluorescence is quantitatively consistent with a single energy transfer pathway from donor to acceptor.

As observed in our earlier work, the decays are generally biexponential, with a small (~10%) long-lived component whose decay is close to that of the isolated donor in solution (4.9 ns). [30]In fitting the donor decay data in Figure 3, we set the long component to be 4.9 ns in all cases. The origin of this long-lived component is not clear, but may be due to a small fraction of impurities not detectable by standard characterization techniques. The results of fitting the donor decays are given in Table 1. Note that the EET times for the fully decorated dendrimers **F** in toluene are faster than those tabulated in our

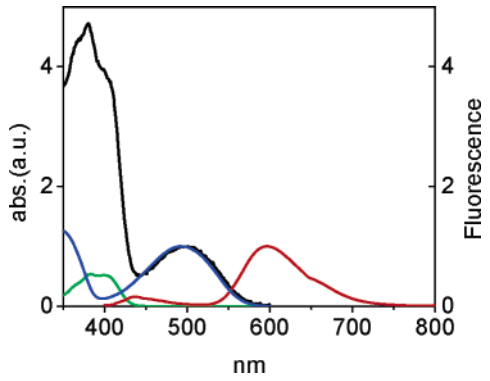

Figure 2. Normalized absorbance of amino-pyrene donor-OH (green), the benzthiadiazole acceptor (blue), and the dendrimer **2F** (black) in toluene, along with normalized fluorescence of **2F** (red) excited at 400 nm. The absorption spectra have been scaled to the absorption coefficient maximum of the acceptor near 500 nm.

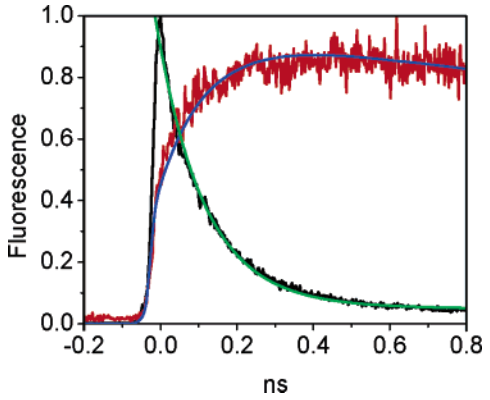

Figure 3. Time evolution of the fluorescence of the donor (black) and acceptor (red) of **3L** in toluene excited at 400 nm. Donor fluorescence is detected in the range of 430−500 nm while the acceptor fluorescence is detected in the range of 560−610 nm. The green and blue lines are the fits to the donor and acceptor data respectively, using the time constants from Table 1.

TABLE 1: Time Dependent Fluorescence Intensity, *I*(*t*), of the Donor Only (Excited at 400 nm) and the Calculated Energy Transfer Time, τ_{EET} from Eq 2[a]

	A_1	τ_1	A_2	τ_2	τ_{EET}		A_1	τ_1	A_2	τ_2	τ_{EET}
1L	0.95	0.040	0.05	4.94	0.040	**3D**	0.85	0.146	0.15	4.94	0.150
2L	0.96	0.075	0.04	4.94	0.076	**1F**	0.95	0.038	0.05	4.94	0.038
3L	0.93	0.124	0.07	4.94	0.127	**2F**	0.96	0.065	0.04	4.94	0.066
1D	0.95	0.044	0.05	4.94	0.044	**3F**	0.92	0.099	0.08	4.94	0.101
2D	0.88	0.079	0.12	4.94	0.080						

[a] The decays are fit to a biexponential form, $I(t) = A_1 \exp(t/\tau_1) + A_2 \exp(t/\tau_2)$, and τ_2 is held constant at $\tau_2 = \tau_D = 4.94$ ns, the fluorescence lifetime of the donor-OH in toluene. All times are in nanoseconds. The standard deviations for τ_1 are all within ±2% of the nominal values.

previous paper, where the lifetimes were measured in DMF. The Forster energy transfer rate is proportional to $1/n^4$,[36] and if we assume that the value for n should be that of the solvent,[37] we can plug in the refractive indices of toluene ($n = 1.494$) and DMF ($n = 1.427$). In this case, we find that the τ_{EET} in toluene should be 20% longer, the opposite of what is observed. An alternative explanation for the more rapid EET in toluene is that the conformational structure, or degree of folding, is slightly different in these two solvents. It is reasonable that toluene could lead to a more compact structure given the polar nature of the BE framework used here.[38] The fact that the fluorescence lifetime of the isolated donor, τ_D, decreases from 9.88 ns in DMF to 4.94 ns in toluene indicates that there are solvent effects on the donor which may also complicate any simple analysis of the absolute value of τ_{EET}.

In the following, we assume that the dominant τ_1 decay component reflects the EET process, and obtain τ_{EET} from the relation

$$\frac{1}{\tau_{EET}} = \frac{1}{\tau_1} - \frac{1}{\tau_D} \qquad (2)$$

where τ_D is the fluorescence lifetime of the isolated donor in toluene. As expected, τ_{EET} increases with increasing generation, and a similar increase is observed within all three families of molecules. Similar trends are also observed in the chemically distinct solvents methylene chloride and DMF. The τ_{EET} values reported in Table 1 differ by at most 50% if we compare the **3D** and **3F** dendrimers. Although a 50% change in τ_{EET} is significant, it actually represents a relatively small change in R (less than 10%) if we assume that the EET follows the R^6 dependence predicted by Forster theory. The fact that there are only slight differences between the **L**, **D**, and **F** families indicates that there are not huge conformational changes between these classes of molecules. The differences in EET times that are observed can be qualitatively rationalized in terms of the different structures. The multibranched **D** dendrimers are consistently slower than the **L** dendrimers, possibly due to greater steric congestion which constrains the donor arms to be more extended. Of course, such steric factors would be even more pronounced in the **F** dendrimers, but here the EET is more rapid than in either disubstituted family. The faster EET in the **F** dendrimers could result from the ability of the many peripheral donor chromophores to transfer energy between each other before transferring it to the core. Donor-to-donor hopping of the excitation would enhance EET to the core by sampling different R distances and/or different orientations. Such donor−donor energy hopping has previously been used to explain efficient EET in other dendrimers.[39,40] If the extra chromophores present in the **F** molecules enable energy hopping and enhance the EET rate, then the EET would be impacted by the number of chromophores as well as their distance from the acceptor.

To analyze whether energy hopping between donors plays a significant role in the EET dynamics, we looked at the evolution of the donor fluorescence anisotropy. We find that attaching the diarylaminopyrene to the first generation benzyl ether dendrimers increases the rotational diffusion time from 80 ps for the isolated donor to ∼130 ps for the first generation molecules. Even in the smallest dendrimer, the effective molecular radius is expected to change by at least a factor of 3, assuming a rigid molecule. The lack of a corresponding decrease in the anisotropy decay rate indicates that the flexible benzyl ether linker probably constrains the motion of the diarylaminopyrene to some extent, but that it can still rotate more or less freely. The anisotropy decay parameters for all the compounds studied are given in Table 2. The anisotropy decays show little dependence on generation in all three families, with the largest effect being a slowdown from 120 to 180 ps for **1D** to **3D**. In the fully decorated dendrimers, the decay actually accelerates with increasing size, with **1F** having a 150 ps decay time, and **3F** having a 120 ps decay. Figure 4 compares the anisotropy decays of **3L**, **3D**, and **3F**, which vary from 180 to 120 ps. The more rapid decay in **3F** suggests that energy hopping between the peripheral donors may be occurring in this molecule. In all dendrimers, however, the anisotropy decays are comparable to the EET times, suggesting that even in the **F** dendrimers there

TABLE 2: Time Dependent Donor Anisotropy, $r(t)$, Fit with a Single Exponential of the Form $r(t) = r_0 \exp[-t/\tau] + y_0$[a]

	r_0	τ	y_0		r_0	τ	y_0
1L	0.315	0.126	0.050	**3D**	0.268	0.180	0.028
2L	0.412	0.119	0.042	**1F**	0.295	0.151	0.056
3L	0.290	0.135	0.016	**2F**	0.314	0.134	0.053
1D	0.388	0.118	0.032	**3F**	0.249	0.115	0.050
2D	0.342	0.178	0.047	donor-OH	0.427	0.082	0.000

[a] All times are in nanoseconds. The standard deviations for all τ are within ±5% of the nominal values.

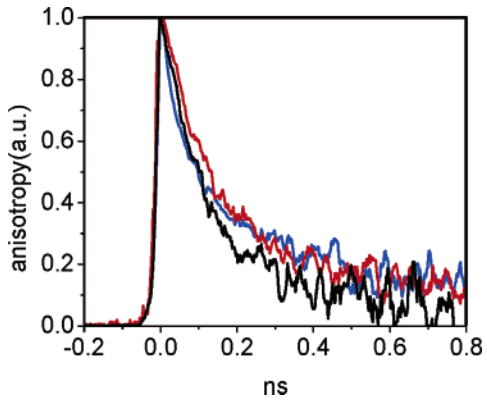

Figure 4. Normalized anisotropy decays of the donor fluorescence for **3L** (black), **3D** (red), and **3F** (blue) molecules in toluene.

is little opportunity to hop to another donor before transfer to the core. This is consistent with the fact that the Forster radius for amino-pyrene-to-benzthiadiazole EET is 4.8 nm, but that for amino-pyrene-to-amino-pyrene is calculated to be only 2.4 nm. The fact that the anisotropy is too slow to significantly impact the EET suggests that donor−donor hopping does not play a significant role in the overall EET dynamics of these molecules. Thus the shorter τ_{EET} values for the **F** dendrimers are just as likely to result from more compact conformations as from energy hopping between donors.

We can understand the dependence of τ_{EET} on molecular generation G by using a simple theory based on flexible polymers. In flexible macromolecules, the average donor−acceptor distance R is expected to scale as the square root of the number of intervening bonds,[41] which can simply be counted from Figure 1. Assuming 8 bonds from the benzthiadiazole center to the ether linkage, and then counting bonds up to the phenyl group of the terminal diarylamino-pyrene donor, we obtain

$$R = A\sqrt{15 + 5G} \tag{3}$$

where A is a constant of proportionality. If the EET occurs mainly via the Forster mechanism, then

$$\tau_{EET} = \tau_D \frac{R^6}{R_0{}^6} = \frac{\tau_D}{R_0{}^6} 125A^6(3+G)^3 = \text{const} \times (3+G)^3 \tag{4}$$

where τ_D is the fluorescence lifetime of the donor in the absence of an acceptor and R_0 is the Forster radius. From fitting the τ_{EET} data as a function of G, and using the values $\tau_D = 4.94$ ns and $R_0 = 4.8$ nm, we can obtain a value for the constant $A = 0.48$ nm. This relation predicts that τ_{EET}, obtained by analysis of the donor fluorescence decay, should increase as $(3 + G)^3$ in a flexible dendrimer system. This conclusion is similar to that obtained for bichromophoric coumarin molecules,[42] and

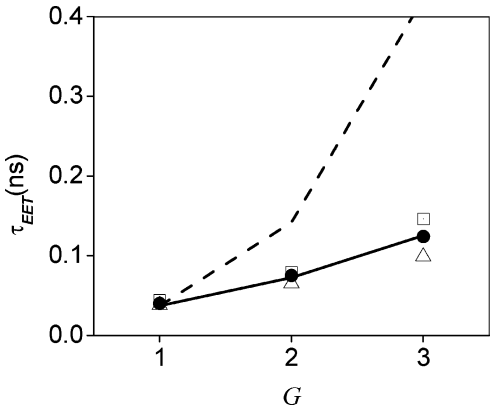

Figure 5. Trend of energy transfer time, τ_{EET}, versus generation for **L** (linear, filled circles), **D** (difunctionalized, open squares), and **F** (fully decorated, open triangles) dendrimers. The $(G + 3)^3$ (solid) and $(G + 3)^6$ (dashed) lines are shown normalized to the **1L** value, where G is the generation number.

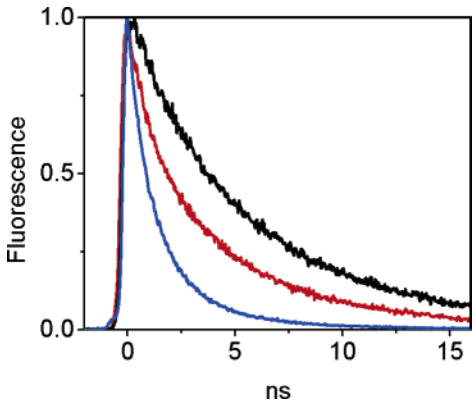

Figure 6. Normalized acceptor fluorescence decay of **3F** in toluene (black), methylene chloride (red), and DMF (blue) excited at 400 nm. The fluorescence in toluene and methylene chloride is detected in the range of 550−730 nm while the fluorescence in DMF is detected in the range of 560−740 nm.

Figure 5 shows that eq 4 provides a good description of the **L**, **D**, and **F** data. A model in which R is assumed to be linearly proportional to the number of intervening bonds predicts that τ_{EET} depends on $(3 + G)$,[6] which clearly overestimates the G dependence of τ_{EET} shown in Figure 5. Other models for relating R to the number of bonds per generation give similar results: the cubic scaling of τ_{EET} with G does not depend on the exact form of eq 3. Other types of experiments have shown that the extension of the dendrimer arms depends sensitively on its chemical structure and the solvent conditions,[43] and that the dependence of R on G can be sublinear.[44]

2. Charge Transfer. Once the core benzthiadiazole has been promoted to its excited state, it can oxidize a ground-state amino-pyrene.[30] This CT event quenches the acceptor fluorescence, and this quenching provides a way to measure the CT kinetics. As the solvent polarity increases, the CT becomes more energetically favorable and the benzthiadiazole fluorescence decay becomes more rapid, as shown in Figure 6. It has been shown for **1F**−**3F** that this fluorescence quenching is accompanied by the formation of a long-lived, charge-separated species.[30] Thus at least part of the rapid fluorescence decay represents CT quenching. Although the monomeric acceptor and the unquenched molecules in toluene yield monoexponential fluorescence decays, as the solvent polarity increases the decays become progressively more nonexponential. This tendency is

TABLE 3: Time Dependent Acceptor Fluorescence Intensity, $I(t)$ (Excited at 400 nm), Fit with a Stretched Exponential of the Form $I(t) \propto \exp[-(t/\tau)^{\alpha}]$[a]

	toluene			methylene chloride			DMF		
	τ	α	τ_{CT}^{dend}	τ	α	τ_{CT}^{dend}	τ	α	τ_{CT}^{dend}
acceptor	6.55	1		8.01	1		7.58	1	
1L	6.49	0.98	1.49E+04	4.62	0.91	12.18	3.11	0.91	5.70
2L	6.48	0.98	3.30E+03	4.53	0.91	11.60	3.37	0.95	6.33
3L	6.48	0.98	3.30E+03	4.6	0.91	12.05	3.84	0.98	7.92
1D	6.35	0.98	291	4.55	0.9	11.90	3.18	0.94	5.75
2D	5.76	0.92	70	4.45	0.89	11.44	3.53	0.91	7.20
3D	6.62	0.98	∞	5.34	0.94	17.48	3.81	0.89	8.62
1F	6.36	0.98	314	3.4	0.81	7.30	1.98	0.88	2.92
2F	6.46	0.98	1.29E+03	2.93	0.75	6.18	1.44	0.85	1.97
3F	5.14	0.86	36	2.81	0.71	6.25	1.28	0.75	1.91
1F (100° C)							0.902	0.88	1.10
2F (100° C)							0.684	0.85	0.83
3F (100° C)							0.798	0.75	1.09

[a] The experimental charge transfer time, τ_{CT}^{dend}, is calculated using eq 7. All times are in nanoseconds. The standard deviations for τ and α are all within ±2% of the nominal values.

most pronounced for the **F** family. To fit these nonexponential decays, we used a stretched exponential function of the type

$$I(t) = I(0)\exp\left[-\left(\frac{t}{\tau}\right)^{\alpha}\right] \tag{5}$$

where τ and α are variable parameters. The stretched exponential function is widely used to describe fluorescence decays when there exists a heterogeneous distribution of decay channels.[45−47] In the present case, it is probably conformational disorder due to the flexible BE arms that leads to a distribution of CT times and the stretched exponential decay for the ensemble. The observed decays can be fit equally well with a biexponential function, but since such a fit involves 3 independently adjustable parameters, as opposed to only 2 with the stretched exponential, we decided to use eq 5 to fit all the acceptor decay data. Table 3 summarizes the results for this fitting for all three families of compounds in the solvents toluene, methylene chloride, and DMF. Table 3 also gives the dendrimer charge transfer time τ_{CT}^{dend} which can be obtained by extracting the average lifetime, $\langle\tau\rangle$, of the stretched exponential decay,

$$\langle\tau\rangle = \frac{\int_0^{\infty} I(t)\,dt}{I_0} \tag{6}$$

and the relation

$$\frac{1}{\tau_{CT}^{dend}} = \frac{1}{\langle\tau\rangle} - \frac{1}{\tau_{acc}} \tag{7}$$

where τ_{acc} is the lifetime of the acceptor in the absence of quenching. The experimental τ_{CT}^{dend} we obtain in this way should be regarded not as resulting from a single CT event but rather as an averaged value which parametrizes the overall CT dynamics.

If we first examine the CT dynamics within a generation, comparing the **L**, **D**, and **F** molecules, we find that the fully decorated dendrimers always exhibit more rapid CT. This is illustrated in Figure 7 for $G = 3$ in DMF. **3L** and **3D** give rise to decays that are close to monoexponential, although they are almost a factor of 2 more rapid than in the nonpolar solvent toluene. The fact that **3D** is slightly slower than **3L** can be rationalized by the extra steric hindrance of backfolding by the dendrimer arms, as in the case of EET. **3F** undergoes a much more rapid decay in DMF, and that decay is clearly nonexponential. The value of $\alpha = 0.75$ suggests that significant heterogeneity exists in the **3F** population, but the lifetime is also much shorter than in **3L** or **3D**. The conclusion is that the extra peripheral donor chromophores in **3F** lead to more rapid CT but also to more disorder than in the disubstituted **L** and **D** analogues.

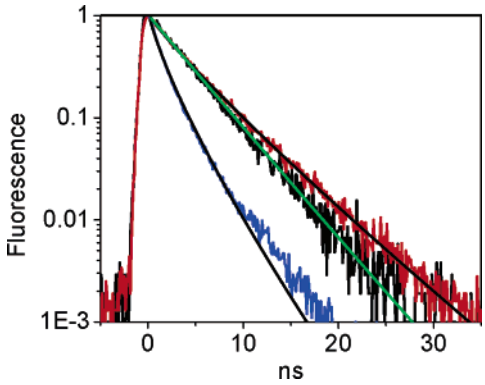

Figure 7. Normalized acceptor fluorescence decays of **3L** (black), **3D** (red), and **3F** (blue) in DMF along with the stretched exponential fits for **3L** (green), **3D** (black), and **3F** (black).

To confirm that conformational dynamics play a role in the observed acceptor decays, we varied the solvent temperature. Raising the temperature should increase both the number of available conformations of the BE arms and their rate of interconversion. Indeed, raising the temperature from 20 °C to 100 °C in DMF increased the fluorescence decay rates by about a factor of 2. This data is shown for **3F** and **3D** in Figure 8. The fluorescence decay of the acceptor by itself does not change over this temperature range. The increase in the decay rate is most pronounced for **3L**, and least pronounced for the **F** compounds. It is not surprising that the **L** and **D** compounds are better able to take advantage of the greater conformational freedom at higher temperatures. First, since they lack all the peripheral chromophores of the **F** dendrimers, they are subject to fewer steric constraints. Second, the greater number of donors in the **F** dendrimers means that, even at room temperature, there are probably conformations which already have a donor in close proximity to the acceptor, so there is less benefit from raising the temperature to populate other conformations. What this data clearly shows is that the acceptor decay dynamics depend sensitively on the details of the conformations and their fluctuations, rather than being the result of a single conformer or geometrical arrangement.

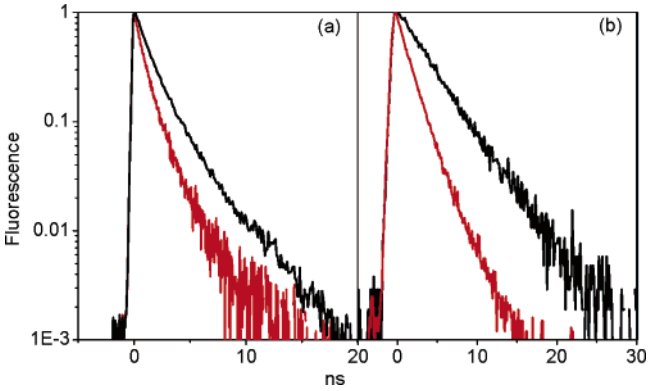

Figure 8. (a) Normalized acceptor fluorescence decays of **3F** in DMF at 20 °C (black) and at 100 °C (red). (b) Normalized acceptor fluorescence decays of **3L** in DMF at 20 °C (black) and at 100 °C (red).

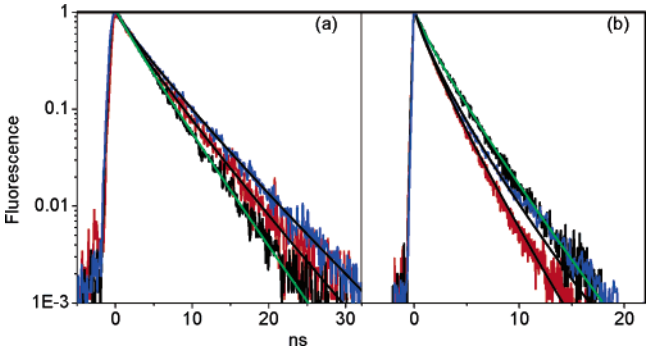

Figure 9. (a) Normalized acceptor fluorescence decays of **1D** (black), **2D** (red), and **3D** (blue) in DMF along with the stretched exponential fits for **1D** (green), **2D** (black), and **3D** (black). (b) Normalized acceptor fluorescence decays of **1F** (black), **2F** (red), and **3F** (blue) in DMF along with the stretched exponential fits for **1F** (green), **2F** (black), and **3F** (black).

The dependence of the CT dynamics on generation is also different for the **F** compounds as compared to the **L** and **D** compounds. Figure 9 compares the decays for **1D**, **2D**, and **3D** in DMF with those of **1F**, **2F**, and **3F**. In the **D** compounds, as in the **L** compounds, the amount of CT quenching decreases as the generation increases. This decrease is relatively small: the observed fluorescence lifetime increases by about 10% on average per generation, but it is above the measurement noise, which is on the order of 2%. As in the case of EET, this behavior in the disubstituted compounds can be rationalized in terms of increasing separation between the donor and acceptor. But this line of reasoning cannot explain the trend seen in the **F** compounds, where the CT quenching becomes more rapid in generations 2 and 3. The change in decay from **2F** to **3F** is especially puzzling. The lifetime decreases, leading to a faster initial fluorescence decay for **3F**, but the smaller value of α also leads to a more pronounced tail in the decay. Thus τ_{CT}^{dend} appears to become shorter as G increases, in contrast to the **L** and **D** compounds, but this increased CT rate is partially obscured by the increased disorder in the **F** compounds. This unexpected result, which can be discerned from both Table 3 and Figure 9, cannot be easily explained in terms of backfolding or more rapid conformational fluctuations. Such effects would be expected to be solvent-dependent, with toluene giving rise to different trends than DMF. But this trend is robust with respect to solvent, which suggests that it is not an artifact of specific conformations but rather results from a global averaging over all conformations. A more reasonable explanation for the decrease in τ_{CT}^{dend} relies on the presence of additional chromophores in the **F** dendrimers which counteract the effect of increasing R on the CT rate, as discussed above. Such an increase in the local concentration of chromophores is absent in the **L** and **D** molecules.

The most interesting question raised by the CT data is why the fully decorated **F** compounds behave so differently from the disubstituted **L** and **D** compounds. A detailed model to explain this divergent behavior would clearly have to take the conformational disorder and dynamic fluctuations of the BE framework into account in order to reproduce the stretched-exponential decays and temperature dependence. Such a model is beyond the scope of this paper. Nevertheless, we can derive a simple model that provides a qualitative explanation for the origin of the observed differences. In the fully decorated **F** dendrimers, the number of available electron donors scales exponentially with generation G:

$$N_{don} = 2^{(G+1)} \tag{8}$$

The distance dependent CT rate for a single donor−acceptor pair is usually taken to be an exponential function of donor−acceptor separation R,

$$k_{CT} = \frac{1}{\tau_{CT}} = k^{(0)}\, e^{-\beta R} \tag{9}$$

The constant β determines the falloff in the electron transfer rate with increasing distance R between donor and acceptor. Equation 9 only considers a single donor−acceptor pair, however, and there are N_{eff} electron donors in a dendrimer of generation G. To take into account the possibility that not all of the available donors can participate equally in the CT, we scale the number of effective donors by a constant b, where $b = 1.0$ implies that all eligible donors participate, while $b < 1.0$ implies that there is some screening of the donor−acceptor interaction. In this case we obtain

$$\frac{1}{\tau_{CT}^{dend}} = N_{eff} k_{CT} = (2b)^{G+1} k^{(0)}\, e^{-\beta R} \tag{10}$$

Using eqs 10 and 3 we obtain

$$\frac{1}{\tau_{CT}^{dend}} = \text{const} \times \exp[\ln(2b)G - \beta A\sqrt{5}\sqrt{3+G}] \tag{11}$$

In eq 11, the constants A, b, and β are all undetermined and thus the detailed behavior of τ_{CT}^{dend} is difficult to predict. But the presence of competing G and $(3 + G)^{1/2}$ terms in the exponent means that this rate must eventually increase with G, or equivalently that τ_{CT}^{dend} will decrease. This is the opposite of the expected behavior of τ_{EET} with increasing G. We emphasize that this model is very simplified and does not take into account complications such as conformational disorder, other types of distance-dependent EET and CT processes, and possible interactions between peripheral donors. Nevertheless, it serves to illustrate how the effects of increasing N_{don} and R can compete with each other in determining how the overall CT rate $1/\tau_{CT}^{dend}$ scales with generation number G. Even though eq 11 does not take some important details of our experiment into account, it is instructive to use it to fit our data. In Figure 10, we plot τ_{CT}^{dend}, obtained from eqs 6 and 7 and the data in Table 3, versus G. We vary the parameters b and β to fit all three sets of data. The fits shown in Figure 10 are obtained for $b = 0.74$ and $\beta = 0.78$ nm^{-1}. For completely unscreened donors, where each has

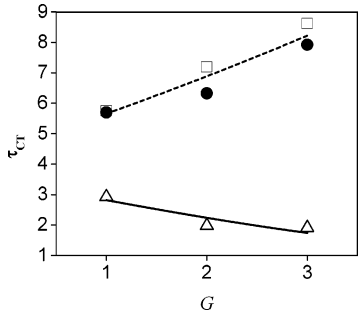

Figure 10. Measured charge transfer times (τ_{CT}) versus size for linear (filled circles), difunctionalized (open squares), and fully decorated (open triangles) dendrimers. The fit to the τ_{CT} of the linear and decorated dendrimers (dashed line) is obtained using the expression $\tau_{CT} \propto \exp[\beta A\sqrt{15+5G}]$, where G is the generation number and $A = 0.48$ nm. The value of A is obtained from Figure 4 using eq 4, $\tau_{EET} = (\tau_{fl}/R_0^6)$-$125A^6(G+3)^3$, where $\tau_{fl} = 4.94$ ns is the fluorescence lifetime of the donor-OH in toluene, and $R_0 = 4.8$ nm is the Forster radius between the donor and acceptor units. The fit to the τ_{CT} of the fully decorated dendrimers (solid line) is obtained using eq 11, $\tau_{CT} \propto \exp[-\ln(2b)G + \beta A\sqrt{15+5G}]$, where the value of $\beta = 0.78$ nm^{-1} obtained from the previous fit, is held constant. The fitting gave $b = 0.74$.

complete access to the acceptor, we would expect $b = 1.0$. Since $b < 1$, this suggests that the number of effective donors does not quite scale exactly with the number of amino-pyrene moieties. The value for β is significantly lower than the range of values that are typically observed for electron transfer reactions (5−12 nm^{-1}).[48] The reason for the low value for β is unclear, but it may reflect the dynamic fluctuations of the BE arms, which was demonstrated by the temperature dependence of the fluorescence quenching. If diffusive motion of the donors leads to changes in their distance from the acceptor during its lifetime, the distance dependence will be blurred, since both short and long arms will eventually undergo a close encounter with the acceptor. Despite its limitations, this simplified model highlights how the competition between size and density in a dendrimer can lead to very different trends with size depending on the physical process studied.

Conclusions

In summary, we have designed, synthesized, and studied three different families of molecules to evaluate how the dendrimer architecture affects the size scaling of the EET and CT dynamics in BE macromolecules. We find that the nature of the branching and the number of peripheral donor chromophores has little effect on how the EET time scales with size. While the absolute EET times can vary by as much as 50% between families, they all exhibit the same general scaling of τ_{EET} with increasing generation G. The CT dynamics, however, show a clear divergence between the behavior of the **L** and **D** molecules, where the number of donors is held constant at $N_{don} = 2$, and the fully decorated **F** dendrimers where $N_{don} = 2^{(G+1)}$. While the CT times for the **L** and **D** molecules increase with generation, as expected due to increasing R, those of the **F** dendrimers actually decrease. In the case of CT, the increase in donor density with generation in the **F** dendrimers apparently alleviates the effect of increasing average donor−acceptor distance. This feature is complicated by the increased conformational disorder in the larger **F** dendrimers, as illustrated by the increasingly nonexponential acceptor fluorescence decays. Despite these complications, our observations have implications for the design of more complicated light-harvesting and charge-separation molecules. In particular, for BE dendrimers it suggests that their flexibility may alleviate some of the decrease in CT and EET rates expected to occur as the size of the dendrimers increases. The key to maintaining a fast CT rate in larger dendrimers may be the ability of the dendrimer framework to increase the local density of the peripheral groups more quickly than the average distance between them and the central acceptor increases.

Acknowledgment. This work was supported by the National Science Foundation, Grant CHE-0517095 (C.J.B.), and by the Basic Energy Sciences of the U.S. Department of Energy, DEFG-02ER15270 (C.J.B.) and DEFG-02ER15503 (S.T.).

References and Notes

(1) Wasielewski, M. R. *Chem. Rev.* **1992**, *92*, 435−461.
(2) Gust, D.; Moore, T. A.; Moore, A. L. *Acc. Chem. Res.* **2001**, *34*, 40−48.
(3) Devadoss, C.; Bharathi, P.; Moore, J. S. *J. Am. Chem. Soc.* **1996**, *118*, 9635−9644.
(4) Stewart, G. M.; Fox, M. A. *J. Am. Chem. Soc.* **1996**, *118*, 4354−4360.
(5) Pan, Y.; Lu, M.; Peng, Z.; Melinger, J. S. *J. Org. Chem.* **2003**, *68*, 6952−6958.
(6) Melinger, J. S.; Pan, Y.; Kleiman, V. D.; Peng, Z.; Davis, B. L.; McMorrow, D.; Lu, M. *J. Am. Chem. Soc.* **2002**, *124*, 12002−12012.
(7) Atas, E.; Peng, Z.; Kleiman, V. D. *J. Phys. Chem. B* **2005**, *109*, 13553−13560.
(8) Meskers, S. C. J.; Bender, M.; Hubner, J.; Romanovskii, Y. V.; Oestreich, M.; Schenning, A. P. H. J.; Meijer, E. W.; Bassler, H. *J. Phys. Chem. A* **2001**, *105*, 10220−10229.
(9) Yeow, E. K. L.; Ghiggino, K. P.; Reek, J. N. H.; Crossley, M. J.; Bosman, A. W.; Schenning, A. P. H. J.; Meijer, E. W. *J. Phys. Chem. B* **2000**, *104*, 2596−2606.
(10) Wagner, R. W.; Johnson, T. E.; Lindsey, J. S. *J. Am. Chem. Soc.* **1996**, *118*, 1166−1180.
(11) Tomizaki, K.; Loewe, R. S.; Kirmaier, C.; Schwartz, J. K.; Restek, J. L.; Bocian, D. F.; Holten, D.; Lindsey, J. S. *J. Org. Chem.* **2002**, *67*, 6519−6534.
(12) Choi, M.-S.; Aida, T.; Yamazaki, T.; Yamazaki, I. *Chem.—Eur. J.* **2002**, *8*, 2668−2678.
(13) Hahn, U.; Gorka, M.; Vogtle, F.; Vicinelli, V.; Ceroni, P.; Maestri, M.; Balzani, V. *Angew. Chem., Int. Ed.* **2002**, *41*, 3595−3598.
(14) Zhou, X.; Tyson, D. S.; Castellano, F. N. *Angew. Chem., Int. Ed.* **2000**, *39*, 4301−4305.
(15) Lu, D.; Feyter, S. D.; Cotlet, M.; Stefan, A.; Wiesler, U.-M.; Herrman, A.; Grebel-Koehler, D.; Qu, J.; Mullen, K.; Schryver, F. C. D. *Macromolecules* **2003**, *36*, 5918−5925.
(16) Metivier, R.; Kulzer, F.; Weil, T.; Mullen, K.; Basche, T. *J. Am. Chem. Soc.* **2004**, *126*, 14634−14635.
(17) Ranasinghe, M. I.; Varnavski, O. P.; Pawlas, J.; Hauck, S. I.; Louie, J.; Hartwig, J. F.; Goodson, T. *J. Am. Chem. Soc.* **2002**, *124*, 6520−6521.
(18) Varnavski, O.; Samuel, I. D. W.; Palsson, L.-O.; Beavington, R.; Burn, P. L.; Goodson, T. *J. Chem. Phys.* **2002**, *116*, 8893−8903.
(19) Gilat, S. L.; Adronov, A.; Frechet, J. M. J. *Angew. Chem., Int. Ed.* **1999**, *38*, 1422−1427.
(20) Serin, J. M.; Brousmiche, D. W.; Frechet, J. M. J. *Chem. Commun.* **2002**, 2605−2607.
(21) Neuwahl, F. V. R.; Righini, R.; Adronov, A.; Malenfant, P. R. L.; Frechet, J. M. J. *J. Phys. Chem. B* **2001**, *105*, 1307−1312.
(22) Adronov, A.; Gilat, S. L.; Frechet, J. M. J.; Ohta, K.; Neuwahl, F. V. R.; Fleming, G. R. *J. Am. Chem. Soc.* **2000**, *122*, 1175−1185.
(23) Andronov, A.; Frechet, J. M. J. *Chem. Commun.* **2000**, 1701−1710.
(24) Balzani, V.; Ceroni, P.; Maestri, M.; Vicinelli, V. *Curr. Opin. Chem. Biol.* **2003**, *7*, 657−665.
(25) Lor, M.; Thielemans, J.; Viaene, L.; Cotlet, M.; Hofkens, J.; Weil, T.; Hampel, C.; Mullen, K.; Verhoeven, J. W.; Auweraer, M. v. d.; Deschryver, F. C. *J. Am. Chem. Soc.* **2002**, *124*, 9918−9925.
(26) Qu, J.; Pschirer, N. G.; Liu, D.; Stefan, A.; DeSchryver, F. C.; Mullen, K. *Chem.—Eur. J.* **2004**, *10*, 528−537.
(27) Ghaddar, T. H.; Wishard, J. F.; Thompson, D. W.; Whitesell, J. K.; Fox, M. A. *J. Am. Chem. Soc.* **2002**, *124*, 8285−8289.
(28) Braun, M.; Atalick, S.; Guldi, D. M.; Lanig, H.; Brettreich, M.; Burghardt, S.; Hatzimarinaki, M.; Ravanelli, E.; Prato, M.; Eldik, R. v.; Hirsch, A. *Chem.—Eur. J.* **2003**, *9*, 3867−3875.
(29) Gutierrrez-Nava, M.; Accorsi, G.; Masson, P.; Armaroli, N.; Nierengarten, J.-F. *Chem.—Eur. J.* **2004**, *10*, 5076−5086.
(30) Thomas, K. R. J.; Thompson, A. L.; Sivakumar, A. V.; Bardeen, C. J.; Thayumanavan, S. *J. Am. Chem. Soc.* **2005**, *127*, 373−383.
(31) Wooley, K. L.; Klug, C. A.; Tasaki, K.; Schaefer, J. *J. Am. Chem. Soc.* **1997**, *119*, 53−58.

(32) Kao, H. M.; Stefamescu, A. D.; Wooley, K. L.; Schaefer, J. *Macromolecules* **2000**, *33*, 6214−6216.

(33) Nantalaksakul, A.; Dasari, R. R.; Ahn, T.-S.; Al-Kaysi, R.; Bardeen, C. J.; Thayumanavan, S. *Org. Lett.* **2006**, *8*, 2981−2984.

(34) Lim, S.-H.; Bjorklund, T. G.; Bardeen, C. J. *J. Phys. Chem. B* **2004**, *108*, 4289−4295.

(35) Ahn, T. S.; Thompson, A. L.; Bharathi, P.; Muller, A.; Bardeen, C. J. *J. Phys. Chem. B* **2006**, *110*, 19810−19819.

(36) Forster, T. Delocalized excitation and excitation transfer. In *Modern Quantum Chemistry, Istanbul Lectures*; Sinanoglu, O., Ed.; Academic Press: New York, 1965; Vol. 3, pp 93−137.

(37) Knox, R. S.; Amerongen, H. v. *J. Phys. Chem. B* **2002**, *106*, 5289−5293.

(38) Hawker, C. J.; Wooley, K. L.; Frechet, J. M. J. *J. Am. Chem. Soc.* **1993**, *115*, 4375−4376.

(39) Jiang, D.-L.; Aida, T. *J. Am. Chem. Soc.* **1998**, *120*, 10895−10901.

(40) Maus, M.; De, R.; Lor, M.; Weil, T.; Mitra, S.; Wiesler, U.-M.; Herrmann, A.; Hofkens, J.; Vosch, T.; Mullen, K.; Schryver, F. C. D. *J. Am. Chem. Soc.* **2001**, *123*, 7668−7676.

(41) Tanford, C. *Physical Chemistry of Macromolecules*; Wiley & Sons: New York, 1961.

(42) Valeur, B.; Mugnier, J.; Pouget, J.; Bourson, J.; Santi, F. *J. Phys. Chem.* **1989**, *93*, 6073−6079.

(43) Tande, B. M.; Wagner, N. J.; Mackay, M. E.; Hawker, C. J.; Jeong, M. *Macromolecules* **2001**, *34*, 8580−8585.

(44) Matos, M. S.; Hofkens, J.; Verheijen, W.; Schryver, F. C. D.; Hecht, S.; Pollak, K. W.; Frechet, J. M. J.; Forier, B.; Dehaen, W. *Macromolecules* **2000**, *33*, 2967−2973.

(45) Lakowicz, J. R. *Principles of Fluorescence Spectroscopy*, 2nd ed.; Kluwer: New York, 1999.

(46) Phillips, J. C. *Rep. Prog. Phys.* **1996**, *59*, 1133−1207.

(47) Lee, K. C. B.; Siegel, J.; Webb, S. E. D.; Leveque-Fort, S.; Cole, M. J.; Jones, R.; Dowling, K.; Lever, M. J.; French, P. M. W. *Biophys. J.* **2001**, *81*, 1265−1274.

(48) Barbara, P. F.; Meyer, T. J.; Ratner, M. A. *J. Phys. Chem.* **1996**, *100*, 13148−13168.